Spectral Broadening in Biomolecules

V. Šrajer, K. T. Schomacker, and P. M. Champion
Department of Physics, Northeastern University, Boston, Massachusetts 02115
(Received 22 May 1986)

We have studied the optical line shapes of deoxy myoglobin (Mb) and its ligand-bound form (MbCO). Simulations of the observed line shapes using "transform" and time-correlator techniques show the presence of strong coupling to low-frequency modes in MbCO and substantial *non-Gaussian* inhomogeneous broadening in Mb. The iron-porphyrin disorder parameter in Mb is found to be $\sigma = 0.25$ Å, and the quadratic dependence of the π-π^* electronic excitation energy on the iron coordinates is also determined.

PACS numbers: 87.15.Mi, 33.20.Fb, 33.70.Jg, 87.15.By

Heme proteins form a class of biological molecules that are involved in a wide variety of fundamental life processes. A large chromophore, known as the heme group, is common to these proteins and plays a key role in the various biological functions (e.g., electron transport, catalysis, oxygen storage, and transport). The iron atom, coordinated at the center of the heme group, generally cycles between two oxidation and/or spin states depending on the biological function being performed. In the case of cytochrome *c*, the familiar electron-transport protein, two axial ligands along with the four planar porphyrin nitrogens coordinate the central iron atom in a strong-field octahedral arrangement. The iron atom is quite literally "locked" in place in this system and always maintains the low-spin configuration.

In contrast to cytochrome *c*, the iron atom in the oxgen-storage protein myoglobin maintains its oxidation state at the ferrous level while cycling between the low-spin ($S=0$) ligand bound state and the high-spin ($S=2$) ligand free state. In this study we consider the carbon-monoxide–bound species (MbCO), and the ligand-free "deoxy" state (Mb). This latter state has a five-coordinate iron atom that is displaced by approximately 0.5 Å from the mean heme plane towards the nitrogen atom of the proximal histidine ligand.[1,2]

Previous work on MbCO, involving the kinetics of CO rebinding as a function of temperature,[3] has produced strong experimental evidence for the existence of protein conformational substates. Other spectroscopic probes, involving Mössbauer,[4] x-ray,[5] and far-infrared magnetic resonance,[6] have also displayed evidence of distributions in protein conformation. In the present work we analyze the optical spectra using "transform" and time-correlator techniques[7-10] and then develop a simple model to account for the inhomogeneous broadening found in the deoxy species.

In general, the optical properties of heme proteins are dominated by the broad (~ 2000 cm^{-1}) and intense ($\epsilon \sim 10^5$ mol^{-1} cm^{-1}) near-ultraviolet (~ 400 nm) "Soret" transition. The Soret band is derived from allowed π-π^* electronic excitations of the porphyrin ring and is asymmetrically broadened by the linear (Franck-Condon) coupling of numerous heme normal modes. The situation is quite analogous to the phonon broadening of optical transitions associated with localized defects in crystals (color centers) and much of the original theory is based on early studies of this classic problem.[7,11]

We have recently demonstrated[10] a strategy for the analysis of optical line shapes that is strongly interdependent on the measurement of absolute resonance Raman-scattering cross sections. When the absolute Raman cross sections are known, a simple Kramers-Kronig transform procedure along with the assumption of linear harmonic coupling allows the direct recovery of the electron-nuclear coupling strengths, $\{S_i\}$, of all modes coupled to the resonant excitation. The Raman spectrum also yields the mode frequencies, $\{\tilde{\nu}_i\}$, so that the Franck-Condon broadening can be calculated explicitly by use of time-domain expressions that are exact at all temperatures.[8] The absorption cross section at frequency $\tilde{\nu}$ is given by

$$\sigma_A(\tilde{\nu}) = C_2 \tilde{\nu}\, \mathrm{Im}\Phi(\tilde{\nu}), \tag{1}$$

with

$$\Phi(\tilde{\nu}) = i\int_0^\infty dt \exp(i\tilde{\nu}t - \Gamma t)\eta(t) \tag{2}$$

and the time correlator

$$\eta(t) = \exp(-i\tilde{\nu}_0 t)\exp\{-\textstyle\sum_i S_i[(2\langle n_i\rangle + 1)(1-\cos\tilde{\nu}_i t) + i\sin\tilde{\nu}_i t]\}, \tag{3}$$

where $\tilde{\nu}_0$ is the 0-0 transition frequency (zero-phonon line) and $\{\langle n_i\rangle\}$ are the Bose-Einstein factors. In Eq. (2),

Γ describes the damping of the Soret excitation by electronic nonradiative population decay.

Two additional sources of line broadening are also explored in the analysis. First, we consider a bath of low-frequency modes (such as chromophore librations and/or bulk protein motions) that is directly coupled to the resonant excitation and yet is not observed in the resonance Raman spectrum. The fact that the frequency dependence of the resonance Raman-scattering cross section is described by two amplitudes having opposite phase,

$$\sigma_R(\tilde{\nu},\tilde{\nu}_1) = C_1\tilde{\nu}(\tilde{\nu}-\tilde{\nu}_l)^3(\langle n_l\rangle+1)S_l|\Phi(\tilde{\nu})-\Phi(\tilde{\nu}-\tilde{\nu}_l)|^2, \quad (4)$$

means that weakly coupled low-frequency modes may not be directly observed, as a result of cancellation of the amplitudes as the Raman mode frequency $\tilde{\nu}_l \rightarrow 0$.[9] In order to approximate the presence of the bath, we use an Einstein approximation with an average frequency $\tilde{\nu}_b$, and integrated bath coupling S_b. The presence or absence of the bath is exposed experimentally by careful measurement of the absorption line shape as a function of temperature.[10]

The second additional source of broadening is inhomogeneous effects that can arise from different protein conformations and environments that are imposed on the heme group. Such broadening is usually modeled as a statistical (i.e., Gaussian) distribution of energy levels.

In Fig. 1 we display the Soret transition of the six-coordinate MbCO complex. The high-resolution spectrum ($\times 0.1$) underlying the broad curves is obtained from Eqs. (1)–(3), with $\Gamma = 10$ cm^{-1} for the excited-state damping factor. With the exception of $(\tilde{\nu}_b, S_b)$, the other parameters $\{\tilde{\nu}_l, S_l\}$ are extracted from the resonance Raman spectra (measured on an absolute scale), by use of Eq. (4) and

$$\Phi(\tilde{\nu}) = \frac{1}{\pi}\int_{-\infty}^{\infty}\frac{\epsilon(\tilde{\nu}')}{\tilde{\nu}'(\tilde{\nu}'-\tilde{\nu})}d\tilde{\nu}' + i\frac{\epsilon(\tilde{\nu})}{\tilde{\nu}}, \quad (5)$$

where $\epsilon(\tilde{\nu})$ is the absorption cross section. The broad solid lines in Fig. 1 are the theoretical results obtained by increasing Γ and including low-frequency coupling. The data are artificially scattered in order to allow visu-

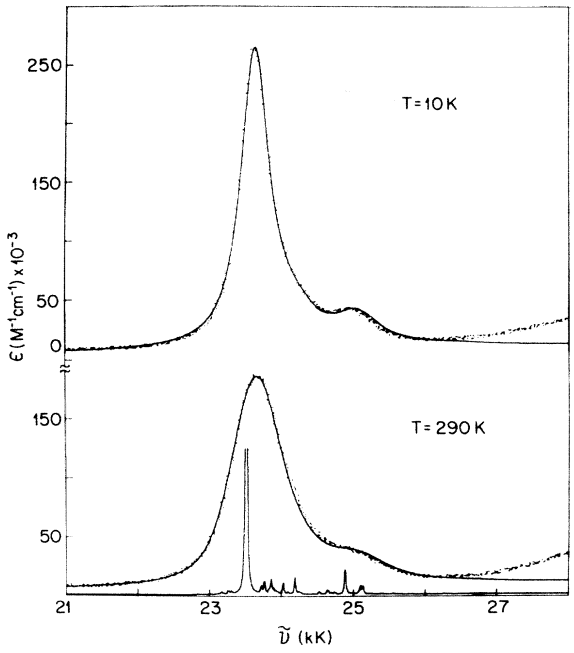

FIG. 1. The experimental Soret bands of MbCO at 10 and 290 K are shown with the solid curves calculated by use of the correlator theory 1 kK (kilokayser) $= 10^3$ cm^{-1}. The fitting parameters Γ and $\tilde{\nu}_0$ are found to be 217 and 23 530 cm^{-1}, respectively. The major reduction in the linewidth observed at low temperature is accounted for by coupling to a low-frequency bath having $\tilde{\nu}_b S_b = 120$ cm^{-1} with $\tilde{\nu}_b < 50$ cm^{-1}.

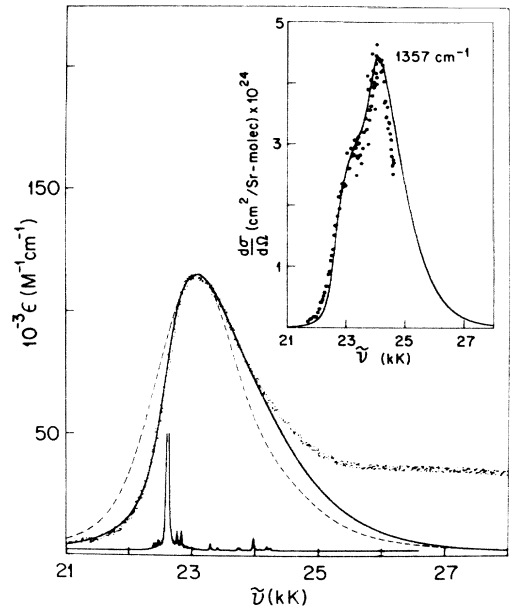

FIG. 2. The experimental Soret band (lower) of deoxy Mb at 290 K is shown with an unsuccessful attempt (dashed line) to fit the data using $\Gamma = 300$ cm^{-1} and a Gaussian inhomogeneous broadening 450 cm^{-1}. A successful fit is generated with $\tilde{\nu}_0 = 22\,630$ cm^{-1}, $\Gamma = 285$ cm^{-1}, and a non-Gaussian inhomogeneous distribution function with $z_0 = 0.5$ Å, $\sigma_z = 0.25$ Å, and $b_z = 2570$ cm^{-1}/Å^2 (solid line). The coupling strengths are again found from the transform analysis and refined to account for the inhomogeneous distribution. When the same distribution is used to calculate the Raman excitation profile of the 1357-cm^{-1} mode (inset) a distinct improvement over the simple transformed absorption band (Ref. 12) is evident.

al differentiation of the theoretical and experimental curves.

It is important to notice in Fig. 1 that a major reduction in the Soret-band linewidth takes place at low temperature. The magnitude of this effect in MbCO is much more pronounced than found for cytochrome *c* and cannot be explained simply by thermal depopulation of the observed low-frequency modes. Thus, the Soret transition of MbCO must involve coupling to a previously unobserved low-frequency subspace. The parameters leading to the best fits of the MbCO spectra are given in the figure caption. It should be noted that the low-frequency mode coupling in MbCO is at least an order of magnitude larger than found for ferrocytochrome *c*.[10]

Our attempts to fit the observed asymmetric broadening of the deoxy Mb spectrum, using these same techniques, proved unsuccessful. When the broadening parameters are increased to account for the overall width of the spectrum, a severe mismatch in the low-energy region is inevitable (see dashed line in Fig. 2). These results have led us to reexamine the nature of inhomogeneous broadening in heme protein optical spectra.

We suggest that stochastic environmental perturbations due to the surroundings of the heme may *not* be primarily responsible for the modulation of the π-π^* electronic excitation energy. Rather, it may be disorder in the position and orientation of the central iron atom with respect to the heme plane that determines the π-π^* energy distribution. Since the iron *d* electrons interact at close range with the π electrons of the porphyrin ring, we might expect this to be a dominant source of inhomogeneous broadening. In the six coordinate compounds the iron-porphyrin distribution is narrow as found for both cytochrome *c* and MbCO. In the five-coordinate deoxy complex it is likely that the iron atom is more loosely bound and the relative mean square displacement in its *z* coordinate (position of the iron atom along the normal to the plane) may be substantial. Additional distributions in the orientational space, as defined by the vector connecting the iron and histidine nitrogen, can also be imagined. Such distributions, may involve the "tilt" of the polar angle (θ) and/or the "rotation" of the azimuthal angle (ϕ) with respect to the heme normal and the porphyrin nitrogen atoms. The azimuthal degree of freedom is of particular interest, since it has been implicated as a source of numerous Raman observations[12] and a wide range of angles ($\phi \sim 0°$–$20°$) is clearly accessible.[1,2]

Given that all three coordinates (z,θ,ϕ) may have importance, we write a general expression for the π-π^* excitation energy:

$$E(Q) \cong E_0 + bQ^2, \tag{6}$$

where Q represents a generalized iron coordinate (z, θ, or ϕ), E_0 is the zero-order π-π^* excitation energy, and b is a constant describing how the coordinates of the iron atom affect the first-order π-π^* excitation energy, $E(Q)$. Only even powers of Q are retained in the expansion because of the approximate reflection symmetry that exists between the iron atom and the porphyrin ring [$E(Q) \cong E(-Q)$]. If we now assume a Gaussian distribution in coordinate space, we find, using Eq. (6), a *non-Gaussian* distribution of electronic energy levels:

$$P(E) = \frac{[(E-E_0)2\pi b]^{-1/2}}{2\sigma}\left[\exp\left(-\frac{[(E-E_0)^{1/2}-Q_0\sqrt{b}\,]^2}{2b\sigma^2}\right)+\exp\left(-\frac{[(E-E_0)^{1/2}+Q_0\sqrt{b}\,]^2}{2b\sigma^2}\right)\right], \tag{7}$$

where Q_0 is the mean coordinate position (e.g., $z_0 = 0.5$ Å) and σ is the disorder parameter of the Gaussian distribution.

When Eq. (7) is employed in the fitting procedure, excellent agreement with the absorption line shape is obtained, as can be seen in the lower portion of Fig. 2 (a separate transition, the "*N*" band at 27×10^3 cm^{-2} is not fitted with this theory). The effects of the inhomogeneous broadening are also reflected in the Raman excitation profile (REP). When the ensemble average used for the absorption band is included in the REP calculation, good agreement with the data is obtained (Fig. 2, inset). This result should be contrasted with the calculations in Ref. 12 which do not include inhomogeneous broadening and are flawed by a 200-cm^{-1} red shift of the theoretical REP maximum. This is particularly compelling evidence for the non-Gaussian energy distribution, since all other attempts to fit the REP using Gaussian distributions, non-Condon effects, etc., have been unsatisfactory.

We have listed the fitting parameters in terms of the iron atom displacement coordinate (z), since this is the most commonly considered degree of freedom in these systems. We hold $z_0 = 0.5$ Å to accommodate the x-ray results and let σ_z and b_z vary to achieve the best fits. Alternatively, one can interpret the results in terms of the orientational degrees of freedom (θ,ϕ). For example, if we again fix the mean coordinate position using the x-ray results, $\phi_0 \cong 20°$, then the fitting parameters become $\sigma_\phi \cong 10°$, $b_\phi \cong 1.44$ cm^{-1}/deg^2.

In z space alone the disorder parameter, $\sigma_z = 0.25$ Å, is somewhat larger than might be expected from EXAFS (extended x-ray absorption fine structure) esti-

mates. However, the value for σ is in excellent agreement with the Mössbauer and x-ray crystallography studies.[5] However, since EXAFS is not generally sensitive to the angular degrees of freedom, we believe that the value found for σ may be a reasonable estimate of the overall disorder (displacement and orientational) of the iron atom with respect to the porphyrin ring.

The parameter b is a measure of how the π-π^* energy gap responds to changes in the iron atom coordinates. For example, the value $b_z = 2570$ cm^{-1}/Å^2 indicates that a ~ 25-cm^{-1} (~ 0.5 nm) blue shift of the Soret band accompanies a 0.1-Å movement of the iron atom away from the heme plane. This value of b is in remarkable agreement with the early calculations of Hopfield[13] which yield

$$\left.\frac{dV(z)}{dz}\right|_{z_0} = 2bz_0 = +0.4 \text{ eV/Å} \cong 3200 \text{ cm}^{-1}/\text{Å},$$

where $V(z)$ is the energy of the optical transition as a function of the iron coordinate, and $z_0 = 0.5$ Å.

It has been known for some time that changes in hemoglobin structure, from the low-affinity "T" to the high-affinity "R" conformation, result in alterations of the Soret band position and shape. These spectral shifts are extremely difficult to quantify, as a result of the presence of four heme groups, not all of which necessarily undergo the same spectral changes during the $T \rightarrow R$ transition.[14] At this stage we only comment that the overall magnitude of the Soret-band red shift accompanying the $T \rightarrow R$ transition is consistent with our value for b if a ~ 0.05–0.1-Å motion of the iron atoms toward the heme plane takes place in the α chains only.[14]

In summary, we have demonstrated how optical line-shape analysis of MbCO as a function of temperature indicates little or no inhomogeneous broadening but does suggest relatively strong coupling to low-frequency modes. The behavior observed for MbCO stands in marked contrast to cytochrome c, which has strong covalent attachments between the heme group and the protein macromolecule. Thus, the low-frequency coupling in MbCO may involve torsions or librations of the unrestrained heme chromophore as well as motions of the CO ligand on a predissociative potential surface prior to photodissociation. The present study has also demonstrated that significant non-Gaussian inhomogeneous broadening is able to explain the deoxy Mb spectra at 290 K. Such broadening may be characteristic of the loosely bound iron atom found in the five-coordinate heme complexes.

The rather large value found for the disorder parameter in the deoxy species is in accord with the nonexponential rebinding kinetics described by Austin *et al.*,[3] provided that one recognizes that the relative iron-porphyrin coordinates can affect the potential energy surfaces relevant to the ligand binding process. A more detailed theory is needed in order to relate quantitatively the distributions of the π electron energy levels discussed here with the distributions in rebinding barrier heights described previously.[3] Preliminary work along this line is encouraging and may yield information about the magnitude of the forces involved in returning the iron atom to the heme center as the ligand binds.

This work is supported by the National Science Foundation (Grant No. 84-17712) and the National Institutes of Health (Grants No. AM-35090 and No. AM-01405).

[1]T. Takano, J. Mol. Biol. **110**, 569 (1977).
[2]S. E. V. Phillips, J. Mol. Biol. **142**, 531 (1980).
[3]R. H. Austin, K. Beeson, L. Eisenstein, H. Frauenfelder, I. C. Gunsalus, and V. P. Marshall, Phys. Rev. Lett. **32**, 403 (1974).
[4]K. Spartalian, G. Lang, and T. Yonetani, Biochim. Biophys. Acta. **428**, 281 (1976).
[5]H. Fraenfelder, G. Petsko, and D. Tsernoglou, Nature (London) **280**, 558 (1979).
[6]P. M. Champion and A. J. Sievers, J. Chem. Phys. **72**, 1569 (1980).
[7]V. Hiznyakov and I. Tehver, Phys. Status Solidi **21**, 755 (1967).
[8]C. K. Chan and J. B. Page, Chem. Phys. Lett. **104**, 609 (1984).
[9]K. T. Schomacker, O. Bangcharoenpaurpong, and P. M. Champion, J. Chem. Phys. **80**, 4701 (1984).
[10]K. T. Schomacker and P. M. Champion, J. Chem. Phys. **84**, 5314 (1986).
[11]M. Lax, J. Chem. Phys. 11, 1752 (1952).
[12]O. Bangcharoenpaurpong, K. T. Schomacker, and P. M. Champion, J. Am. Chem. Soc. **106**, 5688 (1984).
[13]J. J. Hopfield, J. Mol. Biol. **77**, 207 (1973).
[14]J. S. Olson, Proc. Natl. Acad. Sci. U.S.A. **73**, 1140 (1976).